# Fatigue Strength of Small-Defect-Containing Specimens under Combined Loading Involving Phase Difference and Mean Stress

Masahiro Endo[1, a], Isao Ishimoto[2, b], Ken-ichi Iseda[3, c] and Yuki Sakamoto[4,d]

[1, 4] Department of Mechanical Engineering, Fukuoka University,
8-19-1 Nanakuma, Jonan-ku, Fukuoka, 814-0180, Japan

[2] U-Shin Ltd.
1-25-9 Une, Kaita-cho, Aki-gun, Hiroshima 736-0005, Japan

[3] Daikin Industries Ltd.
1304 Kanaoka-cho, Kita-ku, Sakai, Osaka 591-8511, Japan

[a] endo@fukuoka-u.ac.jp, [b] ishimoto105014@u-shin.co.jp, [c] kenichi.iseda@daikin.co.jp,
[d] ysak@fukuoka-u.ac.jp

**Keywords:** Fatigue Strength, Small Defects, Small Cracks, Combined Stress, Mean Stress, Static Stress, Phase Difference, Critical Plane, Criterion, $\sqrt{area}$ Parameter Model, Steels, Brass.

**Abstract.** A unified criterion was proposed for the prediction of the fatigue strength of components containing small holes under combined loading involving the effects of phase difference and mean or static stress. The criterion was based upon the assumption that a Mode I crack on a specific plane, considered a critical plane, plays a dominant role in the determination of fatigue strength. A predictive method for the determination of fatigue strength was also presented making use of this criterion. Combined tension and torsion fatigue tests were conducted using steel and brass specimens containing a small hole of either 100 μm or 500 μm in diameter. The effects of phase difference between tension and torsion, and those of mean or static stress superposed upon the cyclic stress were examined. Non-propagating small cracks emanating from the holes were observed at the fatigue limit. These crack faces coincided approximately with the predicted critical planes. Good agreement between experimental results and predictions of fatigue strength was obtained.

## Introduction

The fatigue strength of engineering components can be lowered by the presence of surface scratches, surface finish flaws, non-metallic inclusions, casting defects, etc. Studies on the influences of such small defects on the fatigue strength under conditions of uniaxial loading have made remarkable progress in the past quarter-century [1, 2]. In many applications, however, engineering components of complex shape, such as suspension parts or crankshafts in automobiles and piping systems with a three-dimensional structure, are usually subjected to multiaxial, cyclic loading involving combinations of bending and torsion. The purposes of this study are to propose a unified criterion that connects the fatigue strength under multiaxial loading with that under uniaxial loading and to give a simple method for the assessment of fatigue strength.

## Criterion and Prediction Method of Fatigue Strength

**Criterion.** Based upon the assumption that the threshold condition for propagation of a Mode I crack is the dominant factor, a unified criterion connecting the uniaxial fatigue strength with the multiaxial fatigue strength was derived [3-5]. The process of the derivation will be briefly reviewed below.

We consider a shaft subjected to combined tension and torsion and then define a rectangular coordinate system, $x$-$y$, on the surface such that the $x$-axis coincides with the axial direction of the shaft and the $y$-axis with the circumferential direction. In the case of a phase difference, $\delta$, between the normal stress, $\sigma_x$, and the torsional shear stress, $\tau_{xy}$, with these stresses having mean stresses of $\sigma_{x,\mathrm{m}}$ and $\tau_{xy,\mathrm{m}}$, the time-variations in $\sigma_x$ and $\tau_{xy}$ at the same frequency are expressed as

$$\sigma_x = \sigma_0 \sin\omega t + \sigma_{x,\mathrm{m}}, \text{ and} \tag{1}$$

$$\tau_{xy} = \tau_0 \sin(\omega t + \delta) \tag{2}$$

where $\sigma_0$ and $\tau_0$ are the amplitudes of the normal stress and the torsional shear stress, respectively, $\omega$ is the angular velocity, and $t$ is the time.

Next, we consider a rectangular coordinate system, $\xi$-$\eta$, in which the $\xi$-axis inclines at an angle of $\theta$ measured counterclockwise from the $x$-axis and assume that a crack emanating from a hole is present on a plane whose normal coincides with the $\xi$-axis and tangent with the $\eta$-axis. The Mode I SIF for a crack under biaxial stresses, $\sigma_\xi$ and $\sigma_\eta$, can be obtained by superposing the effects of each of those stresses acting independently; i.e., the resulting equation is

$$K_{\mathrm{I,biaxial}} = F_{\mathrm{I}\xi}\sigma_\xi\sqrt{\pi c} + F_{\mathrm{I}\eta}\sigma_\eta\sqrt{\pi c} = F_{\mathrm{I}\xi}\Sigma\sqrt{\pi c} \tag{3}$$

where $c$ is the crack length, $\sigma_\xi$ is the normal stress perpendicular to the crack plane, $\sigma_\eta$ is the normal stress parallel to the crack plane, $F_{\mathrm{I}\xi}$ and $F_{\mathrm{I}\eta}$ are the correction factors for the SIF of a crack to which $\sigma_\xi$ or $\sigma_\eta$ is solely applied, respectively, $\Sigma$ is $\sigma_\xi + k\sigma_\eta$, and from Beretta et al.'s calculation [6] $k := F_{\mathrm{I}\eta} / F_{\mathrm{I}\xi} = -0.18$.

The time-variation of $\Sigma$ transformed from Eqs. (1) and (2) is expressed as the following equation which is characterized by an amplitude, $\Sigma_\mathrm{a}$, and a mean value, $\Sigma_\mathrm{m}$, and has a sinusoidal waveform with the same frequency:

$$\Sigma = \Sigma_\mathrm{a}\sin(\omega t + \delta') + \Sigma_\mathrm{m} \tag{4}$$

Details of $\Sigma_\mathrm{a}$, $\Sigma_\mathrm{m}$ and $\delta'$ are given in [5]. Consequently, $K_{\mathrm{I,biaxial}}$ defined by Eq. (3) also has a sinusoidal waveform and its time-variation is given by

$$K_{\mathrm{I,biaxial}} = F_{\mathrm{I}\xi}\sqrt{\pi c}\left[\Sigma_\mathrm{a}\sin(\omega t + \delta') + \Sigma_\mathrm{m}\right] \tag{5}$$

Next, consider another specimen containing a hole of the same size as in the case discussed above for the biaxial stress. When this specimen is subjected to uniaxial cyclic stress with a given mean stress, the value of the SIF for a crack emanating from the hole at the fatigue limit is expressed by

$$K_{\mathrm{I,uniaxial}} = F_{\mathrm{I}\xi}\sqrt{\pi c}\left[\sigma_\mathrm{w}\sin\omega t + \sigma_\mathrm{m}\right] \tag{6}$$

where $\sigma_\mathrm{w}$ is the stress amplitude and $\sigma_\mathrm{m}$ is the mean stress at the uniaxial fatigue limit. If it is assumed that when the time-variation of the SIF under biaxial loading coincides with that under uniaxial loading, the same phenomenon will take place at the tip of a crack, then, on comparing Eq. (5) with Eq. (6), a criterion connecting biaxial fatigue strength with uniaxial fatigue strength can be given as

$$\Sigma_\mathrm{a} = \sigma_\mathrm{w} \text{ and } \Sigma_\mathrm{m} = \sigma_\mathrm{m} \tag{7}$$

If the ranges of $\sigma$ and $\Sigma$ are defined as $\Delta\sigma_\mathrm{w} = 2\sigma_\mathrm{w}$ and $\Delta\Sigma = 2\Sigma_\mathrm{a}$, and the stress ratios as $R = (\sigma_\mathrm{m} - \sigma_\mathrm{w})/(\sigma_\mathrm{m} + \sigma_\mathrm{w})$ and $R_\Sigma = (\Sigma_\mathrm{m} - \Sigma_\mathrm{a})/(\Sigma_\mathrm{m} + \Sigma_\mathrm{a})$, respectively, the criterion of Eq. (7) can be expressed also in the following form:

$$\Delta\Sigma = \Delta\sigma_{\mathrm{w}} \ \text{and} \ R_{\Sigma} = R \tag{8}$$

When applied stresses are sufficiently large the critical condition defined by Eq. (7) or (8) is satisfied for a crack initiated in a wide range of directions of $\xi$-plane, so that the specimen will break. In the actual prediction of fatigue limit, therefore, we need to specify a critical plane that satisfies the criterion exclusively.

The criterion was initially proposed based upon fracture mechanics considerations, but in final form it contains no crack length and has only stress as a variable. Thus, if only the uniaxial fatigue limit, a stress value, is obtained for the material containing a hole concerned in the assessment, the prediction of fatigue strength under combined loading can be made without needing to consider the lengths of any non-propagating cracks.

**Prediction Method.** In predicting the fatigue strength, the uniaxial fatigue limit, $\sigma_{\mathrm{w}}$ or $\Delta\sigma_{\mathrm{w}}$, must first be given as a function of $\sigma_{\mathrm{m}}$ or $R$. This relation can be obtained in a high-cycle fatigue test using specimens containing a small hole with definite dimensions. However, this kind of fatigue test is time-consuming and requires a skilled testing technique. In contrast, the following equation [2] proposed in terms of the $\sqrt{area}$ parameter model is much more convenient for practical use because no fatigue test is necessary.

$$\sigma_{\mathrm{w}} = \frac{1.43(HV+120)}{(\sqrt{area})^{1/6}} \cdot \left[\frac{1-R}{2}\right]^{\alpha} \tag{9}$$

where $\sigma_{\mathrm{w}}$ is in MPa, $HV$ is the Vickers hardness, $\sqrt{area}$ is, in μm, the square root of the area of a defect or a crack projected onto the plane normal to the maximum tensile stress, and $\alpha = 0.226 + HV \times 10^{-4}$.

The fatigue strength prediction procedure is illustrated below taking brass specimens with a 500 μm diameter hole ($HV$ = 125 and $\sqrt{area}$ = 463 μm) as an example. A thick line shown in Fig. 1 is the fatigue limit line for $\sigma_{\mathrm{w}}$ as a function of $\sigma_{\mathrm{m}}$ under uniaxial loading, which is computed from Eq. (9). Next consider, as an example of problem, predicting the normal stress amplitude at the fatigue limit, $\sigma_{\mathrm{a}}$, when the loading condition is such that a steady shear stress of 70 MPa is superposed on cyclic tension-compression loading at an $R$ of –1, i.e. $\tau_0 = \sigma_{x,\mathrm{m}} = 0$ and $\tau_{xy,\mathrm{m}} = 70$ MPa. At this stage, the orientation of the critical plane is as-yet-unknown. If the values of $\Sigma_{\mathrm{a}}$ and $\Sigma_{\mathrm{m}}$ are computed for all

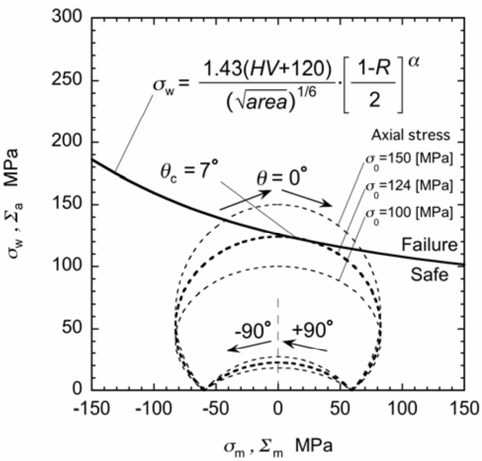


Fig. 1. Illustration of procedure for fatigue limit prediction; high-tension brass, $HV$ = 125, $d = h$ = 500 μm, $\tau_{xy,\mathrm{m}}$ = 70 MPa, $\tau_0 = \sigma_{x,\mathrm{m}} = 0$.

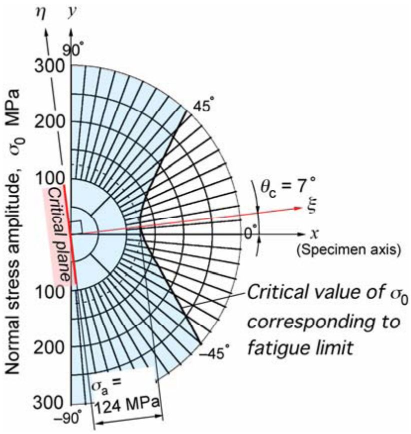


Fig. 2. Critical value of $\sigma_0$ for fatigue limit as a function of $\theta$, the angle between normal of $\xi$-plane and specimen axis.

angles of the $\xi$-axis, $\theta$, with respect to specimen axis between –90º and 90º for arbitrary values of $\sigma_0$, the relations of $\Sigma_a$ and $\Sigma_m$ result in the dashed lines as shown in Fig. 1. If the value of $\sigma_0$ is so small that the dashed line is below the thick line, an infinite life is expected, whereas if the dashed line extends over the thick line, fatigue failure is predicted to take place. The point of tangency between dashed and thick lines satisfies the criterion of Eq. (7) and defines the fatigue limit under combined loading. It is hereupon known that the angle, $\theta_c$, of 7° at this point of tangency is the orientation of the critical plane and the value of $\sigma_0$ corresponding to this dashed line, 124 MPa, is the value of $\sigma_a$ to be predicted.

The above prediction procedure can be explained from a different point of view as follows: Figure 2 shows a line of the values of $\sigma_0$ which are calculated as a function of $\theta$ by satisfying the criterion of Eq. (7) or (8). This curve means that the critical value of $\sigma_0$, i.e. a resistance of material for the fatigue limit, for a given stress condition varies with the direction of $\xi$-axis. The minimum value of $\sigma_0$, 124 MPa, is defined as a value of $\sigma_a$ corresponding to the fatigue limit of a specimen and at this point the angle of critical plane, $\theta_c$, is decided to be 7°.

Furthermore, if the values of $\sigma_a$ are predicted for different values of $\tau_{xy,m}$ in the same procedure, $\sigma_a$ can be obtained as a function of $\tau_{xy,m}$.

## Materials and Experimental Procedure

The materials investigated were an annealed 0.37 % carbon steel (JIS S35C), a quenched and tempered Cr-Mo steel (JIS SCM435); and a high-tension brass. The chemical compositions are listed in Table 1 and the mechanical properties in Table 2.

The experimental procedure and results for the fatigue tests under zero-mean loading have previously been reported in detail [4, 5]. In this study, a new series of fatigue tests has been performed to investigate the effects of mean or static stress. Specimens were of a cylindrical shape with the 8.5 mm diameter for steels and the 10 mm diameter for brass. About a 30 μm thickness of the surface layer was removed by electro-polishing and then a small hole was drilled into the surface of specimens. The diameter of the hole, $d$, was equal to the depth, $h$, and was either 100 μm or 500 μm. After drilling, only the SCM435 steel specimens were annealed in vacuum at 600 ºC. All specimens were slightly electro-polished again before fatigue testing.

A servo-hydraulic uniaxial testing machine and a servo-hydraulic combined tension and torsion testing machine were used for fatigue tests. The operating frequency ranged from 30 to 55 Hz. All tests were conducted under load-controlled sinusoidal loading. The fatigue limit was defined by the critical stress condition that a specimen endured $10^7$ cycles.

| Material | C | Si | Mn | P | S | Cu | Ni | Cr | Mo |
|---|---|---|---|---|---|---|---|---|---|
| S35C | 0.37 | 0.21 | 0.65 | 0.019 | 0.017 | 0.13 | 0.06 | 0.14 | - |
| SCM435 | 0.36 | 0.30 | 0.77 | 0.027 | 0.015 | 0.02 | 0.02 | 1.06 | 0.18 |

| Material | Cu | Pb | Fe | Zn | Mn | Al |
|---|---|---|---|---|---|---|
| High tension brass | 59.1 | 0.0030 | 0.0032 | bal. | 0.021 | 0.0047 |

Table. 1 Chemical composition, in wt.%.

| Material | Lower yield point [MPa] | Tensile strength [MPa] | Elongation (%) | *HV* |
|---|---|---|---|---|
| S35C | 328 | 586 | 25.0 | 164 |
| SCM435 | 858 | 948 | 13.6 | 306 |
| High-tension brass | 205 | 480 | 39.3 | 125 |

Table. 2 Mechanical properties.

## Experimental Results and Discussion

**Behavior of Small Cracks near the Threshold Level.** Figures 3(a) and 3(b) show non-propagating cracks observed at the edge of holes just below the fatigue limit of SCM435 specimens under cyclic tension-compression with tensile or compressive mean stress. The direction of those cracks was macroscopically normal to the maximum principal stress, i.e. $\theta = 0°$, and the length tended to be long under compressive mean stress and short under tensile mean stress.

Figures 4 and 5 show the cracks that caused failure just above the fatigue limit of brass specimens. The specimen shown in Fig. 4 was subjected to 90° out-of-phase combined tension and torsion. The specimen in Fig. 5 was subjected to cyclic tension-compression and steady torsion. The predicted critical planes for those loading conditions are in the directions where the angle between the specimen axis and normal of the planes are ±38° and 7°, respectively. The cracks in Figs. 4 and 5 are macroscopically along the predicted critical planes. Under the stress just below fatigue limit,

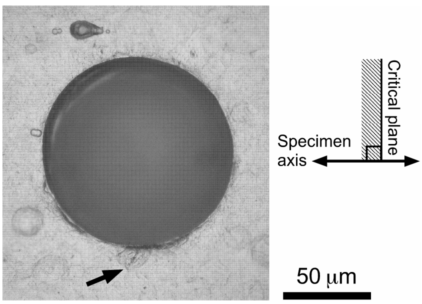


(a) $\sigma_0 = 260$ MPa, $\sigma_{x,m} = 416$ MPa, $\tau_0 = \tau_{xy,m} = 0$.

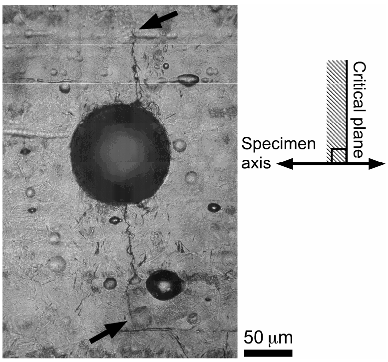


(b) $\sigma_0 = 410$ MPa, $\sigma_{x,m} = -217.6$ MPa, $\tau_0 = \tau_{xy,m} = 0$.

Fig. 3. Non-propagating cracks observed just below fatigue limit under cyclic tension-compression loading with mean tension or mean compression load; SCM435, *HV* = 306, $d = h = 100$ μm.

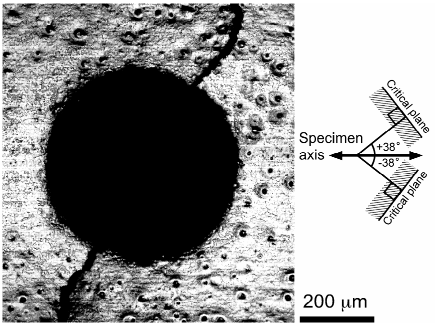


Fig. 4. A crack that caused failure just above fatigue limit under 90° out-of-phase combined tension and torsion loading with no mean load; high-tension brass, $HV$ = 125, $d = h = 500$ μm, $\sigma_0 = \tau_0 = 110$ MPa, $\sigma_{x,m} = \tau_{xy,m} = 0$, $\delta = 90\,^\circ$, $N_f = 5266000$.

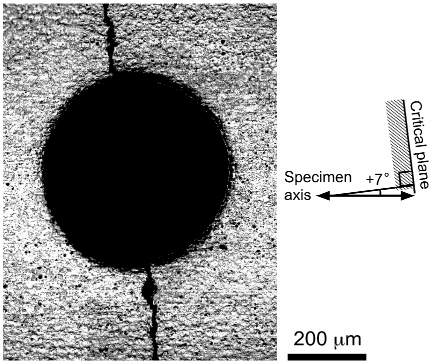


Fig. 5. A crack that caused failure just above fatigue limit under cyclic tension-compression loading with steady torsion; high-tension brass, $HV = 125$, $d = h = 500$ μm, $\sigma_0 = 120$ MPa, $\tau_{xy,m} = 70$ MPa, $\sigma_{x,m} = \tau_0 = 0$, $N_f = 3423000$.

non-propagating cracks were observed approximately along the predicted critical plane. These observations give a basis for the hypothesis that the threshold condition for propagation of a Mode I crack on the critical plane determines dominantly the fatigue strength.

**Comparison of Predicted Results with Experimental Results.** Figure 6 shows a comparison of predicted curves of fatigue limit with the experimental results in the relation between $\sigma_a$ and $\tau_a$ at an $R$ of –1 for the cases of the phase differences of 0º and 90º. In this figure, $\sigma_a$ and $\tau_a$ are normalized by the uniaxial fatigue limit, $\sigma_w$, predicted for $R = -1$ by Eq. (9). It is seen that the experimental fatigue limits are well predicted, regardless of material and hole size.

Figure 7 shows the effects of mean stress or static stress on the fatigue limit. It is seen that good

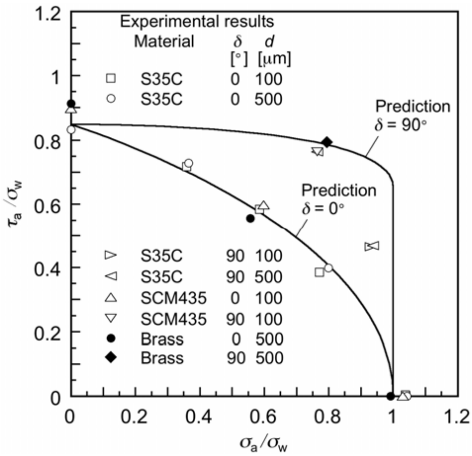


Fig. 6 A comparison of the predictions with the experimental results of fatigue limit under in-phase and 90° out-of-phase loadings at an $R = -1$; $\sigma_a$ and $\tau_a$ are normalized by $\sigma_w$ predicted using Eq. (9).

agreement between experimental and predicted results has been obtained.

The effects of shear-mode loading acting on the plane of a crack initiated on the critical plane is considered to be small within a range of testing conditions investigated in this study. When the phase difference, $\delta$, and their mean stresses are not zero, however, the amplitude, $\Sigma_a$, is no longer constant but it varies with time, with $\Sigma$ having a complex waveform. The fatigue strength prediction for such a case may be out of the range of applicability of the method proposed in this study.

## Conclusions

A criterion and a prediction method for fatigue strength of specimens containing small holes under combined axial and torsional loading have been described. The conclusions can be summarized as follows:

1. Non-propagating small cracks emanating in the radial direction from a hole were observed at the fatigue limit. The fatigue strength is determined by the threshold condition for propagation of a crack initiated on a critical plane determined by the loading conditions.
2. On the assumption that the role of Mode I fatigue loading is dominant, a criterion connecting the uniaxial fatigue strength with the multiaxial fatigue strength was proposed. A practical method for the prediction of fatigue strength was also proposed by use of this criterion and the $\sqrt{area}$ parameter model.
3. Combined axial and torsional loading fatigue tests of annealed JIS S35C steel, quenched and tempered JIS SCM435 steel, and high-tension brass specimens were performed under a variety test conditions involving phase differences and mean stresses. The experimental results for the orientation of the critical plane and the fatigue strength were in good agreement with the predictions.
4. The effects of shear-mode loading acting on the plane of a crack initiated on the critical plane is considered to be small within a range of testing conditions investigated in this study.

## Acknowledgement

This work was in part supported by funds (No. 081501) from the Central Research Institute of Fukuoka University.

## References

[1] Y. Murakami, M. Endo, *International Journal of Fatigue*, Vol. 16 (1994), pp. 163-182

[2] Y. Murakami, *Metal Fatigue: Effects of Small Defects and Nonmetallic Inclusions*, (2000), Elsevier.

[3] M. Endo, *Small Fatigue Cracks: Mechanics, Mechanisms and Applications*, (1999), pp. 375-387, Elsevier.

[4] M. Endo, I. Ishimoto, *Int. J. Fatigue*, Vol. 28 (2006), pp. 592-597

[5] M. Endo, I. Ishimoto, *J. Solid Mechanics and Materials Engineering*, Vol. 1, No. 3 (2007), pp. 343-345

[6] S. Beretta, Y. Murakami, *Fatigue and Fracture of Engineering Materials and Structures*, Vol. 23 (2000), pp. 97-104

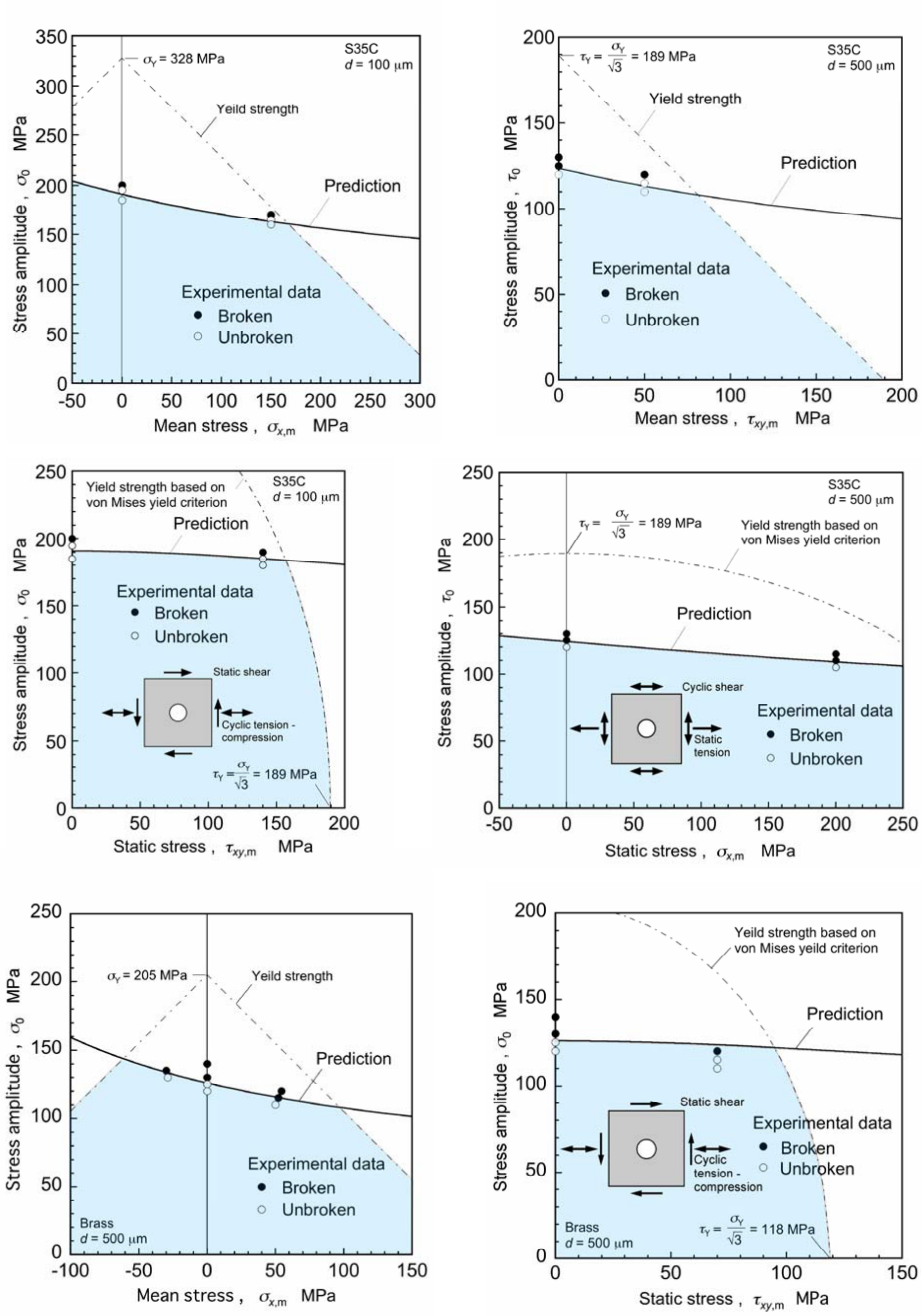

Fig. 7 Comparisons of the predictions with the experimental results of fatigue limit under cyclic loading with mean or static stress; S35C and brass specimens containing a 100 or 500 μm diameter hole.